



**CHALMERS**  
UNIVERSITY OF TECHNOLOGY

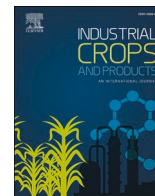
## **Elucidation of cellulose phosphorylation with phytic acid**

Downloaded from: <https://research.chalmers.se>, 2025-04-04 17:26 UTC

Citation for the original published paper (version of record):

Orzan, E., Barrio, A., Spirk, S. et al (2024). Elucidation of cellulose phosphorylation with phytic acid. *Industrial Crops and Products*, 218. <http://dx.doi.org/10.1016/j.indcrop.2024.118858>

N.B. When citing this work, cite the original published paper.



# Elucidation of cellulose phosphorylation with phytic acid

Elliott Orzan<sup>a</sup>, Aitor Barrio<sup>b</sup>, Stefan Spirk<sup>c,\*</sup>, Tiina Nypelö<sup>a,d,\*\*</sup>

<sup>a</sup> Department of Chemistry and Chemical Engineering, Chalmers University of Technology, Kemivägen 10, Gothenburg 412 96, Sweden

<sup>b</sup> TECNALIA, Basque Research and Technology Alliance (BRTA), Área Anardi 5, Azpeitia 20730, Spain

<sup>c</sup> Institute of Bioproducts and Paper Technology, Graz University of Technology, Inffeldgasse 23, Graz 8010, Austria

<sup>d</sup> Department of Bioproducts and Biosystems, Aalto University, Vuorimiehentie 1, Aalto FI-00076, Finland

## ARTICLE INFO

### Keywords:

Natural fiber  
Functionalization  
Condensation reaction mechanism  
Thermal stability  
Flame-retardant  
Cross-link  
Hydrolysis  
Degradation

## ABSTRACT

The worldwide ban on the use of halogenated flame retardants has accelerated the development of non-toxic alternatives from natural feedstock, such as phytic acid. The fire suppressing mechanisms which acidic phosphates impart on cellulosic materials rivals most solutions yet promotes cellulose hydrolysis and degradation. Current attempts to prevent degradation that results from the acid hydrolysis and to improve flame retardancy rely on the use of catalysts without evaluating the effect of curing temperature on cellulose phosphorylation. In this study, the fundamental condensation reaction between cellulose and phytic acid reveals how varying curing temperature affects the phosphorylation and degradation of cellulosic structures. Curing a low concentration of phytic acid on cellulose at 160 °C was shown to promote the phosphorylation of cellulose over the formation of oligo-phosphates. The addition of phytic acid and rise in curing temperature degraded non-crystalline moieties and improved thermo-oxidative stability credit to the char layer formation of the phosphorylated cellulose structure. Increased phosphorus content expectedly led to improved thermal stability, yet cross-linking of phytic acid to cellulose overcame the need for increased phytic acid concentrations. This work thus provides the basis for the application of heat-curing phytic acid at low concentrations to target cellulose fire-retardancy using a chemical catalyst-free and solvent-free approach.

## 1. Introduction

The transition towards applying bio-based materials obtained from renewable resources continues to be an exciting and technical challenge to the world of chemistry. Among those resources, phytic acid has seen a rise in popularity credited to its unique structure and bioavailability. Also known as myo-inositol hexakisphosphate or IP6, phytic acid is extracted from the plant tissues of bran, seeds, and legumes to increase the valorization of waste by-products generated in the processing of these foods. The poly-phosphorylated structure has promoted its use as an anti-microbial agent in agriculture, anti-oxidant in food science, and a potential anti-cancer compound in medicine. (Blout et al., 2021) Importantly, phytic acid has become a promising agent in the creation of bio-based flame-retardant materials. (Guo et al., 2017; Liu et al., 2021, 2018; Song et al., 2022; Zheng et al., 2022)

Phytic acid is primarily thought to act as a charring flame-retardant agent. This implies that the dehydration and cross-linking of acidic phosphates when exposed to heat creates an exterior carbonaceous glass

layer, shielding the material from oxygen and heat in the form of a condensed (solid) phase. (Liu et al., 2021; Price et al., 2001) On the other hand, the formation of gas phase radicals (i.e. PO·) slows down chain reactions of hydrogen and hydroxy radicals, thereby reducing heat propagation. However, due to their dominant action in the condensed phase, phosphates are thought to form fewer radicals in the gas phase than other phosphorus containing compounds. (Schartel, 2010)

The presence of phosphate groups causes phytic acid to be soluble in water, and thus requires some degree of chemical bonding to remain on washable substrates. (Antoun et al., 2022; Barbalini et al., 2019; Liu et al., 2021; Song et al., 2022) An established methodology treats phytic acid and textile fabrics and reacts them with compounds containing amine groups such as melamine and dicyanamide. (Cheng et al., 2022; Feng et al., 2017; Liu et al., 2018; Ren et al., 2022; Sun et al., 2021; Thota et al., 2020; Yuan et al., 2021) The result is strong covalent bonding with improved flame-retardant properties due to the synergy between phosphorus and nitrogen; yet this method requires the use of additional solvents and toxic compounds. A more recent method to

\* Corresponding author.

\*\* Corresponding author at: Department of Chemistry and Chemical Engineering, Chalmers University of Technology, Kemivägen 10, Gothenburg 412 96, Sweden.  
E-mail addresses: [orzan@chalmers.se](mailto:orzan@chalmers.se) (E. Orzan), [aitor.barrio@tecnalia.com](mailto:aitor.barrio@tecnalia.com) (A. Barrio), [stefan.spirk@tugraz.at](mailto:stefan.spirk@tugraz.at) (S. Spirk), [tiina.nypelo@aalto.fi](mailto:tiina.nypelo@aalto.fi) (T. Nypelö).

<https://doi.org/10.1016/j.indcrop.2024.118858>

Received 4 February 2024; Received in revised form 25 May 2024; Accepted 26 May 2024

Available online 8 June 2024

0926-6690/© 2025 The Authors. Published by Elsevier B.V. This is an open access article under the CC BY license (<http://creativecommons.org/licenses/by/4.0/>).

introduce nitrogen has been through the use of ammonium phytate (Cheng et al., 2022; Feng et al., 2017), or reacting urea with phytic acid (Antoun et al., 2022; Feng et al., 2017; Ghanadpour et al., 2015; Liu et al., 2018; Ma et al., 2021; Sun et al., 2021; Yuan et al., 2021) to promote the covalent linking between phytic acid phosphate groups and substrate hydroxyl groups. Introduction of ammonium groups such as urea causes fiber swelling and neutralizes the strong acidity of phytic acid, reducing fiber damage and preventing degradation in material tensile properties. (Cheng et al., 2022; Feng et al., 2017) It has also been suggested that electrostatic potential and hydrogen bonding provides sufficient cross-linking stability when formed via layer-by-layer deposition, although washability has not been verified. (Liu et al., 2022; Ren et al., 2022; Song et al., 2022; Wang et al., 2022; Zheng et al., 2022) Here, we evaluate the formation of covalent ester bonds between acidic phosphates and cellulose by varying curing temperature at a low phytic acid concentration. Phytic acid is known to undergo poly-phosphorylation, however, this work suggests that intra-phosphate bonding may occur at low phytic acid concentrations, leading to the formation of reactive cyclic anhydride groups. (Antoun et al., 2022; Guo et al., 2017; Liu et al., 2021; Xie et al., 2023) This is generally accepted as the mechanism by which citric acid and 1,2,3,4-butanetetracarboxylic acid are cross-linked to wool or cotton fabrics. (Štiglic et al., 2022; Yang et al., 1997) However, the underlying reaction mechanisms and resulting chemical structure of cellulose phosphorylation is not fully explored.

The preferential phosphorylation of cellulose over oligo-phosphorylation is hypothesized to occur via condensation reactions with increasing curing temperatures at low phytic acid concentrations. The interaction of phytic acid with cellulose substrates at varying curing temperatures is elucidated to understand changes in the microstructure and in the thermo-oxidative stability of the material. Here, we suggest the key reaction mechanisms and analyze the morphological and chemical products of this methodology. The sparing use of reactants and the absence of catalysts demonstrates how covalent bonds between the phosphate compounds and cellulose can be formed with acidic phosphates while avoiding the wasting of resources. This will allow the progression of phosphate-based technologies towards imparting flame-retardant properties to OH group containing substrates.

## 2. Experimental

### 2.1. Materials

Whatman Cytiva qualitative filter paper (Grade 5, 47 mm diameter) were purchased from Fisher Scientific (Sweden). Phytic acid solution (50 % w/w in H<sub>2</sub>O) was purchase from Merck (Sweden). All reagents purchased were used without further purification.

### 2.2. Cellulose substrate preparation

Phytic acid solution (0.3 mL of 0.044 M) was evenly spread over each Whatman Cytiva grade 5 qualitative filter paper. Filters were dried at 80 °C for 15 hours in a convection oven. Evaporating the water leads to a theoretical concentration of 5 wt% phytic acid on the filters after drying. Then the filter papers were heat-cured at 20, 80, 120 and 160 °C to mimic conditions used in other studies. (Demitri et al., 2008; Ferreira et al., 2020; Frone et al., 2020; Guo et al., 2017; Meftahi et al., 2018; Ottenhall et al., 2018; Štiglic et al., 2022; Yang et al., 1997) Filters labelled with a W were washed after drying and curing by adding 200 mL DI water, followed by 100 mL 95 % ethanol, and once again washed with 200 mL DI water in a Büchner funnel. The filters were dried again at 80 °C for 1 hour.

Sample nomenclature was designated as follows: P at the start denotes application of phytic acid solution, the number dictates the curing temperature after drying, and the W or U at the end indicates whether the filter was washed or unwashed after curing. P20U and P20W were

never dried at 80 °C, instead dried at room temperature for 2 days.

### 2.3. Nuclear magnetic resonance (NMR) spectroscopy

Solid-state NMR was performed in a 4 mm ZrO<sub>2</sub> MAS rotor with a set temperature of 298 K in all experiments. <sup>13</sup>C CP/MAS NMR spectra were recorded with a MAS rate at 10KHz. <sup>13</sup>C cross-polarization spectra were recorded with a <sup>13</sup>C field of 60.0 kHz and 83 kHz SPINAL-64 1 H decoupling was applied. The <sup>31</sup>P MAS NMR was recorded with a MAS rate of 12.5 kHz. TPPM15 1 H decoupling at 54 kHz was applied with 10 s delay between repetitions and a total of 64 scans. <sup>31</sup>P NMR deconvolution was performed in PeakFit v4.12 by Systat Software GmbH. The baseline was subtracted, and a Gaussian deconvolution was performed.

Crystallinity (CR) was calculated via peak deconvolution of area (A) of cellulose C4 at 89 and 85 ppm for A<sub>crystalline</sub> and A<sub>non-crystalline</sub>, respectively, by fitting a Gaussian curve and determining the area underneath. Eq. 1 was used to calculate the crystallinity. (Zuckerstätter et al., 2009)

$$\text{Cr}(\%) = \frac{A_{\text{crystalline}}}{A_{\text{crystalline}} + A_{\text{non-crystalline}}} * 100 \quad (1)$$

### 2.4. Fourier transform infrared spectroscopy – Attenuated total reflection (FTIR-ATR)

FTIR-ATR spectroscopy was used to investigate the cellulose substrate to determine changes in the molecular structure after application and cross-linking of phytic acid. Substrates were cured, immediately put in a desiccator, and analyzed after 2 days. A PerkinElmer Frontier FTIR spectrometer with PIKE technologies GladiATR measured 32 scans of each substrate 3 times with a data interval of 1 cm<sup>-1</sup> and 4 cm<sup>-1</sup> resolution. The ATR crystal was cleaned with isopropyl alcohol, air-dried and the sample was pressed onto the surface with a mechanical anvil. The scanned wavenumbers were from 400 to 4000 cm<sup>-1</sup>. PerkinElmer Spectrum software was used to correct background noise and all spectra were normalized to the same intensity value at 4000 cm<sup>-1</sup>.

### 2.5. Elemental Analysis

Elemental analysis was performed by MIKROLAB Mikroanalytisches Laboratorium Kolbe (Germany). Phosphorus content determination was done after microwave digestion on a MARS 6 from CEM on a Spectro Model Arcos ICP.

### 2.6. X-ray photoelectron spectroscopy (XPS)

The photoelectron spectra were measured at a PHI Versaprobe III spectrometer employing monochromated Al K $\alpha$  radiation for excitation. A spot of 100×100  $\mu\text{m}$  was illuminated by the X-rays. The spectra were recorded with a 45° take-off angle. The binding energy scale was referenced to the position of the leading peak in the C 1 s signal corresponding to C-O in cellulose and positioned at 286.7 eV. (Johansson et al., 2020) Charge compensation was achieved by simultaneous use of an electron flood gun and an Ar<sup>+</sup> ion source. The spectrometer is routinely calibrated according to ISO 15472:2010. Relative quantification of the elements was done with the MultiPak software (PHI) based on the integral intensity of the signals using sensitivity factors. Peak decomposition was done by fitting a set of Voigt profiles to the spectrum. The width of the Lorentzian part was fixed and the width of the Gaussian part was a free fitting parameter but kept the same for all peaks in a specific spectrum. (Campbell and Papp, 2001) A Shirley type background was subtracted prior to peak fitting.

## 2.7. Scanning electron microscopy (SEM)

The cellulose substrates were sputter-coated with 4 nm of gold before SEM visualization was performed on a JEOL 7800 F Prime at an acceleration voltage of 5 kV.

## 2.8. Thermogravimetric analysis (TGA)

To understand the thermal degradative behaviour of phosphorylated cellulose papers when exposed to heat, TGA analysis was used. A Mettler Toledo TGA/DSC 3+ was utilized to sequence the following heating sequence using STARe Software: 1. Ramp from 30 °C – 500 °C at a rate of 10 K/min under 60 mL/min air flow, 2. Temperature hold at 500 °C for 5 mins, 3. Ramp from 500 °C – 700 °C at a rate of 10 K/min under 60 mL/min air flow, 4. Temperature hold at 800 °C for 10 mins.

The reported values are an average of 3 separately prepared substrates. Carbonization onset was set as the point where the slope of the graph deviated by more than 3 %. Weight loss during carbonization was calculated from this point to where the slope begins levelling out as indicated by a change in slope of 30 %. Finally, residual weight was taken as the weight percent of the material at 700 °C.

## 3. Results and discussion

### 3.1. Phytic acid phosphates undergo condensation reactions to form covalent ester bonds

Condensation reactions or dehydration synthesis involve the esterification of hydroxyl-containing compounds via the elimination of water. In the present method, heat is applied to a system involving phosphates in phytic acid and cellulose hydroxyl groups. To overcome entropic effects, heat or other catalysts are required to run condensation reaction in aqueous media. Heat promotes the removal of water, driving nucleophilic attack from either phytic acid phosphates or cellulose hydroxyl groups. The proposed reaction mechanisms include inter-phosphate (1), intra-phosphate (2) and phosphate-cellulose (3) linkages (Fig. 1) with products depending on the reaction conditions, i.e., phytic acid:cellulose ratio, solvent, and temperature.

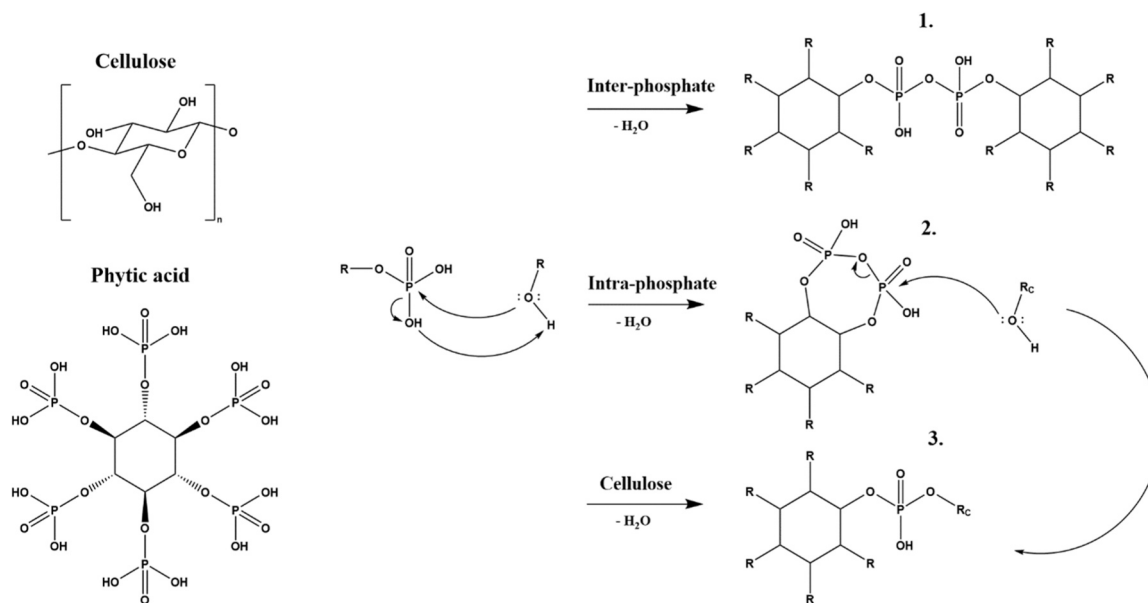


**Fig. 1.** Molecular structures of cellulose and phytic acid with proposed mechanisms for dehydration condensation reactions. Reactants are phosphate groups and either cellulose or another phytic acid molecule where R = either phosphate groups ( $\text{PO}_3\text{-H}$ ) or C2, C3 or C6 of cellulose.  $\text{R}_c$  is defined as specifically C2, C3 or C6 of cellulose. Products 1, 2 and 3 are the proposed products of the reaction, depending on the mechanism of action described above the arrow. Product 2 is a highly reactive cyclic anhydride formed via intra-phosphorylation reactions, likely causing it to react further with cellulose generating product 3 as indicated.

The low electronegativity of phosphorus in phosphate groups is the favored target for nucleophilic attack by both cellulose and other phosphate groups. Hydroxyl groups on phosphates are more nucleophilic than cellulose but must overcome steric constraints. Here, we employ an aqueous solution with a lower concentration (0.04 M in solution, 5 wt% dry) of phytic acid compared to previous studies, preferring the formation of 3. (Antoun et al., 2022; Barbalini et al., 2019; Cheng et al., 2022; Liu et al., 2022, 2018) An intra-phosphorylation reaction between phosphates of the same phytic acid molecule may theoretically occur in dilute systems, leading to the formation of 2. However, the cyclic anhydride nature of this structure is highly reactive, which is susceptible to nucleophilic attack by cellulose OH groups, thereby forming 3. Oligo-phosphated structures may be formed as a result of inter-phosphate reactions, generating polymeric chains as described by the displayed R groups in Fig. 1. (Kokol et al., 2015) Phytic acid may also undergo thermal decomposition via dephosphorylation pathways. (Daneluti and Matos, 2013; Watson et al., 2019) Apart from highly complex mixtures of P1-P5 phytic acid derivatives, it may also create ortho- and pyrophosphates as proven by solution-state  $^{31}\text{P}$  NMR spectroscopy. (Watson et al., 2019)

Solid state  $^{31}\text{P}$  NMR spectroscopy was performed to investigate the outcome of the condensation reaction (Fig. 2a). Literature reports that phytic acid typically yields a single broad peak around 0 ppm in a solid state  $^{31}\text{P}$  NMR spectra. (Antoun et al., 2022; Barbalini et al., 2019; Rol et al., 2020) However, deconvolution of the P20U spectra in Fig. 2a revealed a system of three overlapping peaks at 0.5,  $-0.7$ , and  $-2.0$  ppm (Supporting Information Figure S1). Hydrogen bonding of the phosphate to cellulose caused an upfield shift from 0.5 to  $-0.7$  ppm. The area of the peak at  $-0.7$  ppm changed by less than 1 % between P20U and P160W, indicating that the degree of hydrogen bonding in the system does not change after curing. The downfield peak at 0.5 ppm present in both deconvoluted spectra is characteristic of unreacted phytic acid phosphate mono-esters. Integration of this peak area showed a strong decrease from 48 % to 28 % for P20U and P160W, respectively. The 20 % decrease for P160W reappears as a series of peaks below  $-1.0$  ppm, where the formation of a shoulder in the P160W curve compared to P20U (Supporting Information Figure S2a) represents the successful formation of new ester bonds to phosphorus.

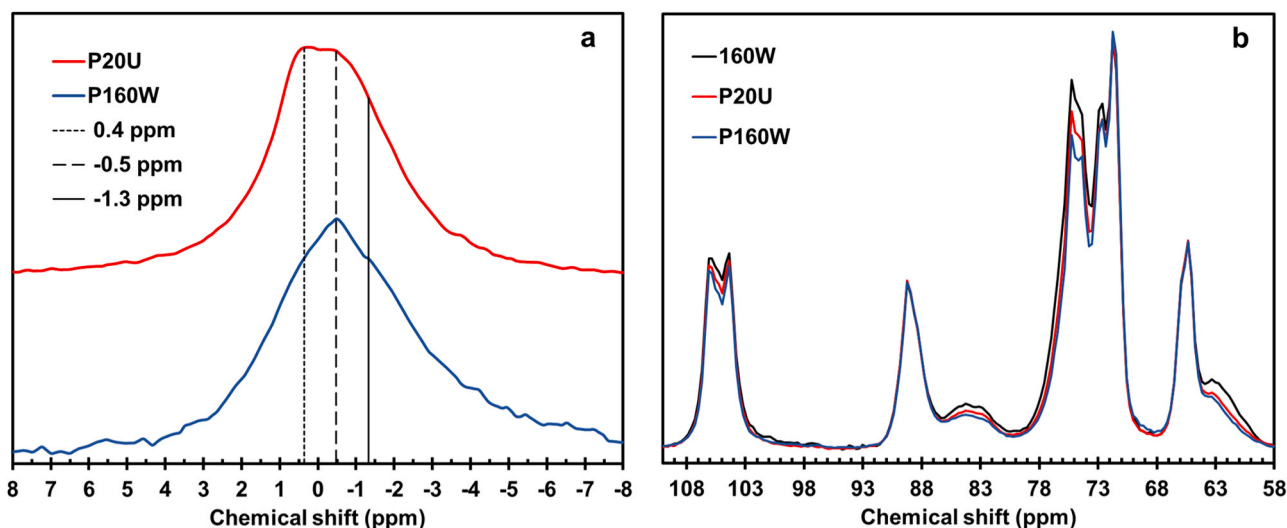


Fig. 2. Solid-state NMR peaks of a)  $^{31}\text{P}$  showing the change in the characteristic peaks at 0.4,  $-0.5$  and  $-1.3$  ppm and b)  $^{13}\text{C}$  showing inconclusive evidence of phosphorylation, yet significant changes in the non-crystalline regions of C4 (84 ppm) and C6 (63 ppm).  $^{31}\text{P}$  NMR peaks were re-scaled to similar intensities and  $^{13}\text{C}$  NMR peaks auto-scaled to match interior crystalline moieties of C4 at 89 ppm and C6 at 65 ppm.

The primary result of the condensation reactions in P160W are phosphate di-esters as suggested by the 24 % area contribution of the  $-2.0$  and  $-3.0$  ppm deconvolution peaks (compared to 13 % for P20U). (Antoun et al., 2022; Ghanadpour et al., 2015; Rol et al., 2020) The small yet distinct peak in the  $^{31}\text{P}$  NMR spectra at  $-1.3$  ppm present for P160W (Fig. 2a) indicates the successful formation of di-ester covalent bonds between cellulose and phytic acid which shield the phosphorus. Peaks further upfield are attributed to oligo-phosphates and tri-esters which have bound to cellulose, accounting for 9 % of the spectra area. On the downfield side of the spectra from 1.5 to 7.5 ppm, negligible differences between the peak areas are observed. This would indicate either a similar or a lack of discernable phytic acid dephosphorylation or degradation into ortho- and pyro-phosphates (Supporting Information Figure S2). Considering the washing step applied to P160W, any of these unbound products would have been removed. The  $^{13}\text{C}$  NMR spectra reveal no significant changes in chemical shifts to support phosphorylation, however, the intensities of certain carbon atoms changed for the phytic acid treated cellulose (Fig. 2b). The phosphates bound to the cellulose chains comprise a small fraction of the total (0.7 wt% in P160W, Table 1) and thus would cause a nearly indiscernible shift.

Analysis of C1s XPS spectra revealed an increased intensity of the C-C peak at about 285 eV for P160W (Supporting Information Figure S3a,b). It has been suggested that this change represents  $\text{HPO}_4$  phosphates coating the surface of the cellulose substrate through phosphorylation, causing either an increase, (Rol et al., 2020) or decrease (Ghanadpour et al., 2015) in intensity. However, the change observed here is instead ascribed to the dephosphorylation of phytic acid, or the presence of contamination. Peaks representing C=O (289.3 eV), O-C-O (288.1 eV), and C-O (286.7 eV) bonding displayed little change due to the relative abundance of cellulose compared to phytic acid moieties. The O1s

spectrum of P160W shows the presence of phosphates on cellulose from P=O bonding at 531.6 eV. O-H bonding at 534.3 eV representing adsorbed  $\text{H}_2\text{O}$  and some hydroxyl groups had an observable decrease in relative intensity to the C-O / P-O peak at 533.2 eV (Supporting Information Figure S3d). In the P2p spectra, the intensity of the P-O bonding at 134.3 eV respective to P=O at 135.2 eV increases after curing phytic acid on cellulose (Supporting Information Figure S4). (Rol et al., 2020; Thota et al., 2020; Wang et al., 2022) Elemental composition of the cellulose substrates measured via XPS suggests that atomic percent of oxygen for both 160 W and P160W is 43.6 %. These results agree with findings by (Rol et al., 2020), yet is unexpected when considering the proposed reactions. The substitution of OH groups on cellulose by phytic acid or phosphates should create a substrate with more OH groups, especially when considering the partial hydrolysis of cellulose causing additional groups to become exposed. Rather, the consistent observation is that OH groups decrease when phytic acid is cured on cellulose substrates at 160 °C. This indicates that the condensation reactions with phosphates at 160 °C removes the OH groups, creating ester bonds in place and phosphorylating cellulose.

FTIR spectroscopy confirms the results from  $^{31}\text{P}$  NMR spectroscopy

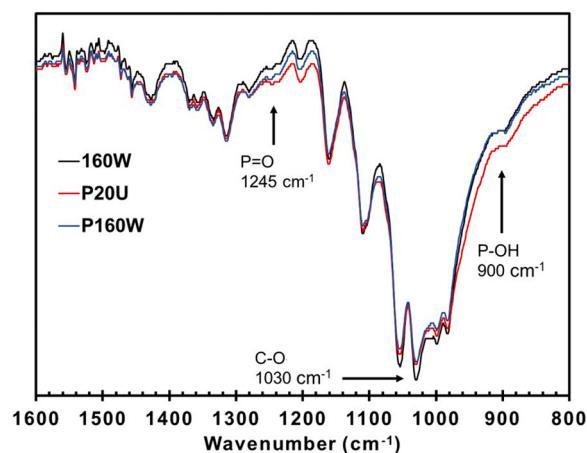


Fig. 3. ATR-FTIR spectrum comparing a blank cellulose substrate exposed to 160 °C curing temperature and washed (160 W), a substrate doped with phytic acid, cured at 160 °C and washed (P160W), and a substrate with phytic acid and dried at RT (P20U).

Table 1

Effect of curing temperature on the phosphorus content and crystallinity of cellulose substrates.

Sample	Phosphorus content (%)		Crystallinity (%)
	Unwashed	Washed	
160	-	-	66
P20	1.78	0.05	70
P80	1.66	0.08	69
P120	1.65	0.27	71
P160	1.42	0.70	72

and XPS (Fig. 3). The band at  $1245\text{ cm}^{-1}$  ( $\delta_{\text{P=O}}$ ) corresponds to the stretching of P=O bonds and represents the amount of phosphates present. (Ghanadpour et al., 2015; Kokol et al., 2015) Upon addition of phytic acid (P20U), the  $1245\text{ cm}^{-1}$  band increased in intensity and later decreased when cured and washed (P160W) as the total amount of phosphorus was lower for P160W than for P20U (Table 1). Normalizing the spectra to the band at  $1245\text{ cm}^{-1}$  and observing the shoulder occurring at  $900\text{ cm}^{-1}$  ( $\delta_{\text{P-OH}}$ ) reveals a decrease in intensity of about 3 % for P160W compared to P20U. This again suggests that on each phosphate, the amount of P-OH bonds has decreased after curing the substrate at  $160\text{ }^\circ\text{C}$  by forming ester bonds as found in  $^{31}\text{P}$  NMR and XPS.

Direct probing of C-O-P bonding in XPS and FTIR is difficult due to issues in differentiating from P-O-H bonding in P2p spectra and C-O-C stretching in FTIR regions from  $980 - 1160\text{ cm}^{-1}$ . In FTIR, this region represents C-O bond vibrations which result from both C-O-C in cellulose and C-O-P due to phosphorylation. The intensities therefore result primarily from cellulose with minor influence from phosphorylation. When applying normalization of the characteristic C-O peaks occurring from  $980$  to  $1160\text{ cm}^{-1}$  ( $1030\text{ cm}^{-1}$  chosen here) to P=O, an increase in intensity of 2 % for P160W over P20U is revealed. This small increase continues to corroborate with observations implying that phosphates have bonded to cellulose.

Therefore, condensation reactions of phytic acid on cellulose are supported by the combination of results from NMR, XPS and FTIR spectra. Nonetheless, given that phytic acid additive has a relatively minor impact on intensity compared to the cellulose, it becomes difficult to statistically discern significant differences. We take our observations of the analysis as indicators building to a similar conclusion.

### 3.2. Phytic acid curing affects cellulose fiber network structure and crystallinity

The application of phytic acid to cellulose fibers caused changes in cellulose crystallinity, substrate morphology and rate of drainage during the washing step. Elemental analysis provided quantification of phosphorus remaining on the substrates after the washing step (Table 1). The decrease of phosphorus content through washing was noticeably lower on substrates treated with higher curing temperatures. This is further reflected by the increasing intensity of the phosphorus signal in  $^{31}\text{P}$  NMR spectra (Figure S2b). Notably, P20W substrates retained little phosphorus, indicating that hydrogen bonding between phosphate and cellulosic hydroxyl groups was insufficiently strong to bind phytic acid to the fiber surfaces. P80W similarly retained little phosphorus, indicating that phosphorylation due to condensation reactions was not achieved at this temperature. However, the unwashed sample P80U had a noticeable decrease in phosphorus content compared to P20U, indicating that phytic acid may have undergone dephosphorylation to gaseous phosphoric acid moieties without reacting with the cellulose substrate. Increasing curing temperature to  $120\text{ }^\circ\text{C}$  and  $160\text{ }^\circ\text{C}$  allowed the retention of phosphorus on the cellulose surface after washing yet also caused unwashed substrates to lose more phosphorus, especially at  $160\text{ }^\circ\text{C}$ . The degradation temperature of phytic acid was shown to be  $150\text{--}160\text{ }^\circ\text{C}$ , thus the decrease of 0.3 % phosphorus from P20U to P160U can be justified by dephosphorylation to gaseous phosphoric acids. (Daneluti and Matos, 2013) However, this does not explain the decrease in phosphorus at  $80\text{ }^\circ\text{C}$ .

The covalent binding of phytic acid molecules to cellulose (Fig. 1) would result in difficulty to remove phosphorus from the cellulose substrate. While covalent bonds to cellulose are proposed as the primary product of this reaction, phytic acid chains may polymerize resulting in the formation of oligo-phosphates. Such structures would have reduced solubility in water and ethanol and could be physically restrained within the cellulose network. This would result in phosphorus retention on the cellulose substrates without needing to covalently bind it to cellulose. Under the presented curing conditions, these oligo-phosphate structures are suggested to covalently bind to cellulose as evidenced by the

presence of upfield peak contributions in the  $^{31}\text{P}$  NMR spectra. By deliberately using low concentrations of phytic acid, the primary product of these condensation reactions would be cellulose phosphorylation to phytic acid with the inevitable generation of some oligo-phosphates.

As an acid, phytic acid expectedly affected the structure of the cellulose substrate. The  $^{13}\text{C}$  NMR spectra show that the intensity of the C4 (non-crystalline) peak at 85 ppm decreased with the application of phytic acid, and furthermore decreased with heat while the C4 peak (crystalline) at 89 ppm remains unchanged (Fig. 2b). These are of particular interest as the C4 atoms are typically used for crystallinity percentage determinations via peak area deconvolution. (Newman, 2004; Wickholm et al., 1998; Zuckerstätter et al., 2009) The application of phytic acid to the cellulose substrate (P20U) increased the crystallinity by 4 %. This increase in crystallinity is not caused by the crystallization of cellulose moieties, but rather from the acid hydrolysis of non-crystalline regions increasing the percentage contribution from crystalline regions. When reaching  $160\text{ }^\circ\text{C}$ , the additional 2 % hydrolysis can be ascribed to the further hydrolysis of these regions by the action of phosphoric acids. Stacked  $^1\text{H}$  NMR,  $^{13}\text{C}$  NMR are also presented in Supporting Information Figure S5.

The non-crystalline region of C4 hides another detail which may reveal the action of phytic acid. The unmodified cellulose substrate contains two minor sharp peaks within the larger broad curve of the non-crystalline peak (Supporting Information Figure S6). Wickholm and Larsson delved into the deconvolution of cellulose I C4 peaks and depicted these minor peaks as the accessible fibril surfaces surrounding interior crystalline regions. (Wickholm et al., 1998; Zuckerstätter et al., 2009) The disappearance of these structures could result from two scenarios: (i) The reduction in outer accessible fibril surfaces by the covalent bonding of phytic acid on cellulose fibrils. The interior regions would thus be a para-crystalline structure linking disparate fibrils. (ii) Hydrolysis of the outer non-crystalline sheaths surrounding crystalline regions, effectively reducing their signal intensity in solid state NMR spectra. Since the entire breadth of the non-crystalline peak decreases, the work of phytic acid is suggested to be cleaving fibrillar structures. As the outer accessible fibril surfaces are degraded, inner inaccessible non-crystalline structures between crystalline regions can be accessed. These inaccessible regions which make up the broad peak are exposed and furthermore degraded, leaving a broad peak which decreases in intensity and has reduced non-crystalline outer regions.

SEM images displayed in Fig. 4 corroborate the idea of fibril degradation action by phytic acid. On a macroscopic level, there appears to be a reduction in the presence of loosely bound cellulose microfibrils when phytic acid is applied and cured. Increasing the curing temperature revealed cracks and folds in the cellulose fibers, which are indicative of acidic action (Fig. 4c). Overall, the SEM images are still difficult to interpret as the dilute concentration of phytic acid had little macroscopic effect; yet these observations are reinforced by similar findings at higher concentrations. (Antoun et al., 2022; Liu et al., 2018; Ma et al., 2021)

These small changes would change the interaction of cellulose fibrils as a network structure. Many studies on the application of phytic acid to fabrics have reported the degradation of mechanical properties with and without the use of catalysts or other modification. (Antoun et al., 2022; Cheng et al., 2019; Feng et al., 2017; Jiang et al., 2012; Liu et al., 2022, 2018; Ma et al., 2021; Song et al., 2022; Sun et al., 2021) P160W was also notably faster at draining than other substrates when washing (P160W: 20 seconds vs P20U: 30 seconds). Therefore, it can be surmised that the addition of a curing step created porosity in the cellulose network by the work of phosphoric acids. The increased porosity may also allow the removal of unbound and insoluble oligo-phosphates which were previously suggested to be retained on the cellulose substrate. Reducing the concentration of phytic acid applied and using the proposed method of phosphorylation may be the answer to form a covalently bound fibrillar network to offset the loss of support

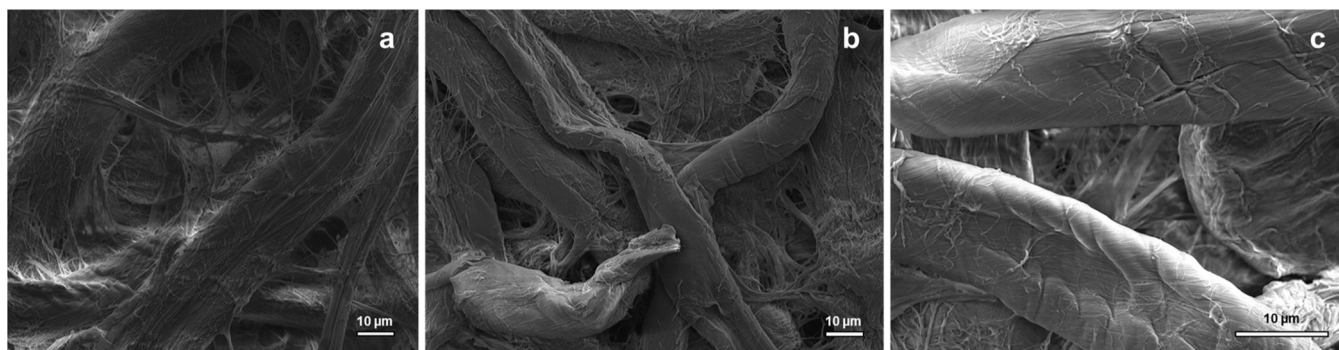


Fig. 4. SEM characterization of a) 160 W, b) P20U, c) P160W. Phytic acid coated substrates labelled with a P present fewer microfibrillar features and more cracking.

structures.

### 3.3. Cellulose phosphorylation retains thermal stability and causes changes in the char layer formation

The flame-retardancy and thermal stability mechanism of phytic acid relies on the presence of phosphorus in the gaseous and condensed phases during pyrolysis. In the gas phase, phosphorus radicals neutralize hydrogen and hydroxy radicals to reduce flame propagation. However, phosphates tend to act primarily in the condensed phase. (Schartel, 2010) As temperature increases, phytic acid begins to decompose, forming phosphoric acids. These acids catalyze the dehydration of cellulose, causing carbonization. Carbonization of cellulose and phytic acid forms a char layer, a stable physical barrier against heat, oxygen, and fiber degradation. (Liu et al., 2021; Price et al., 2001)

The development and function of the char layer could be described with TGA (Fig. 5a). Enhancing the phytic acid content led to the formation of a char layer at reduced temperatures, attributable to the phytic acid's limited thermo-oxidative stability. (Daneluti and Matos, 2013) Ideally, the char layer forms quickly into a closed-cell porous structure to reduce oxygen and thermal diffusion. (Price et al., 2001) The formation of this structure prevents further degradation of the bulk material and reduces weight loss (Table 2). However, the formed char layer was not perfectly insulating, indicated by the gradual reduction in weight after the curve begins to stabilize at 250–300 °C to the onset of combustion at 500 °C (Fig. 5a). The weight loss likely developed as a result of the formation of an open-celled porous structure, which would allow the diffusion of material. (Price et al., 2001) The rate of weight loss in P120W and P160W was slightly increased compared to P20U

which suggests that phosphorus content and the cross-linked phytic acid structure with cellulose influences the formation of the char layer.

Each of the properties listed in Table 2 displayed similar trends to the example of carbonization onset in Fig. 5b. As curing temperature increases, phosphorylation allowed the retention of phosphates on cellulose after washing, which in turn improved the overall thermo-oxidative stability of the material. With unwashed substrates, the carbonization onset gradually rose with increasing curing temperature due to phytic acid degradation. This observation correlates well with the decreasing phosphorus content found in elemental analysis. However, the weight loss of unwashed substrates after carbonization onset remained constant with increasing curing temperature. This suggests that the weight loss does not correlate to phosphorus content but rather to the quality of the char layer formed from cellulose phosphorylation.

The extent to which any thermal stability is retained after washing does not always correlate with the phosphorus content. For example, P160W changed by less than 5 % in carbonization onset compared to P160U albeit a reduction in phosphorus content of nearly 50 %. P20U similarly only had an improvement of 13 % in carbonization onset over P160W albeit having 150 % more phosphorus. Therefore, the cross-linking of phytic acid to cellulose via condensation reactions was able to quickly generate a char layer using less phosphorus. Comparing the weight loss and residual weight of these samples, we can again conclude that the quality of the formed char layer played a more significant role than the quantity of phosphorus applied.

## 4. Conclusion

Curing phytic acid on cellulose substrates at temperatures up to 160

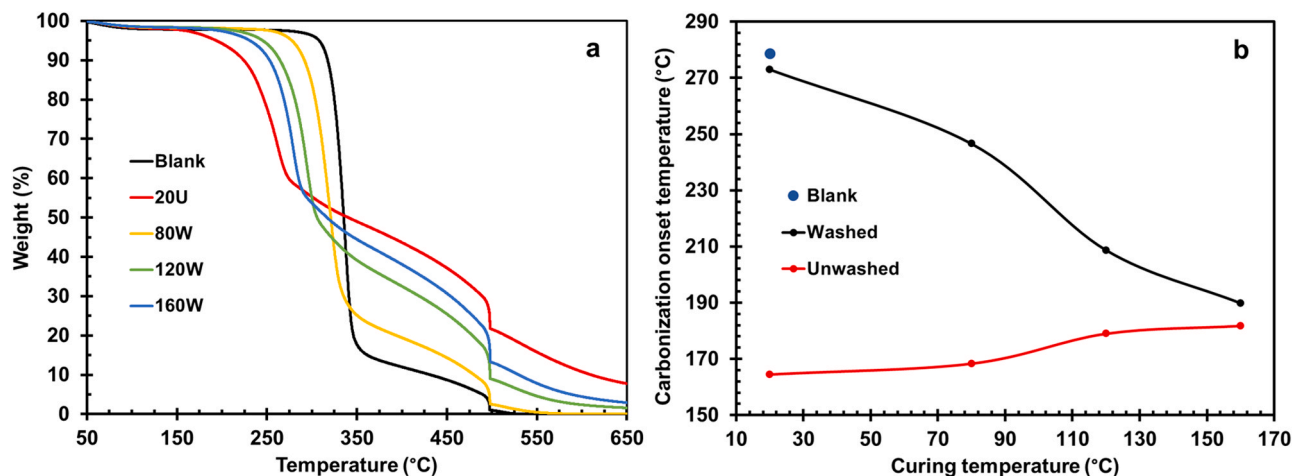


Fig. 5. TGA of cellulose substrates coated with phytic acid showing a) overall TGA curves changing with curing temperature and b) carbonization onset temperature changing with increasing curing temperature and washing step as an example trend of all other thermal stability indicators in TGA.

**Table 2**

TGA of phytic acid coated substrate to determine indicative thermo-oxidative stability.

Property	Blank	P20U	P20W	P80U	P80W	P120U	P120W	P160U	P160W
Carbonization onset temperature (°C)	279	165	273	168	247	179	209	182	190
Degradation weight loss (%)	73	42	72	42	65	42	51	42	43
Combustion onset weight (%)	4	20	5	20	6	18	10	19	16
Residual weight (%)	0	4	1	3	0	3	1	2	2

°C causes increasing phosphorylation as a product of the condensation reactions. The formation of oligo-phosphated structures is typically suggested in literature as the product of this reaction; however, this work proposes the formation of covalent ester bonds between cellulose and phytic acid as the primary product in systems with low phytic acid content. Curing at 160 °C was the most effective temperature for phosphorylation within the chosen conditions. The formation of gaseous phosphoric acids at this temperature reduces phosphorus content and degrades cellulose, yet the subsequent phosphorylation reaction promotes retention of phosphorus on the cellulose fiber surface after washing. The cross-linked structure formed a char layer faster and was as effective at preventing material degradation compared to substrates with more phosphorus.

The drive towards using bio-based materials to functionalize cellulose fibers and fabrics has made phytic acid a viable option for thermal stability and flame-retardancy. This non-toxic compound can be efficiently cross-linked to cellulose via condensation reactions without the use of non-water solvents or toxic catalysts. This work provides the foundation necessary to understand how curing temperature and phytic acid concentration affects the products of cellulosic phosphorylation condensation reactions. With a basic understanding of cellulose phosphorylation, degradation and char layer formation, phytic acid can now reach the next developmental stages in the progress towards applying it to flame-retardant bio-based materials.

#### CRediT authorship contribution statement

**Elliott Orzan:** Writing – review & editing, Writing – original draft, Methodology, Investigation, Formal analysis, Conceptualization. **Aitor Barrio:** Writing – review & editing, Methodology, Investigation. **Stefan Spirk:** Writing – review & editing, Supervision, Methodology, Investigation, Formal analysis. **Tiina Nypelö:** Writing – review & editing, Supervision, Resources, Formal analysis, Conceptualization.

#### Declaration of Competing Interest

The authors declare the following financial interests/personal relationships which may be considered as potential competing interests: Tiina Nypelo reports financial support was provided by European Commission. If there are other authors, they declare that they have no known competing financial interests or personal relationships that could have appeared to influence the work reported in this paper.

#### Data availability

Data will be made available on request.

#### Acknowledgments

The authors would like to thank Andreas Schaefer from Chalmers for providing XPS data collection and analysis and Tobias Sparman of the Swedish NMR center in Umeå, Sweden for their expertise, help and excellence in NMR data collection. Also, thanks to Alex Idström for his help in establishing contacts and ideas. Thank you to Nina Kann for the guidance and support regarding the phosphorus compounds. This work has received funding from the European Union's Horizon 2020 - Research and Innovation Framework Programme under grant

agreement No 964430. Tiina Nypelö acknowledges the funding from Wallenberg Wood Science Center and Area of Advance Materials, Chalmers University of Technology.

#### Appendix A. Supporting information

Supplementary data associated with this article can be found in the online version at [doi:10.1016/j.indcrop.2024.118858](https://doi.org/10.1016/j.indcrop.2024.118858).

#### References

- Antoun, K., Ayadi, M., El Hage, R., Nakhli, M., Sonnier, R., Gardiennet, C., Le Moigne, N., Besserer, A., Brosse, N., 2022. Renewable phosphorus-based flame retardant for lignocellulosic fibers. *Ind. Crops Prod.* **186**, 115265.
- Barbalini, M., Bertolla, L., Tousek, J., Malucelli, G., 2019. Hybrid silica-phytic acid coatings: effect on the thermal stability and flame retardancy of cotton. *Polymers* **11** (10), 1664.
- Bloot, A.P.M., Kalschne, D.L., Amaral, J.A.S., Baraldi, I.J., Canan, C., 2021. A review of phytic acid sources, obtention, and applications. *Food Rev. Int.* 1–20.
- Campbell, J.L., Papp, T., 2001. Widths of the atomic K-N7 levels. *At. Data Nucl. Data Tables* **77** (1), 1–56.
- Cheng, X.-W., Guan, J.-P., Kiekens, P., Yang, X.-H., Tang, R.-C., 2019. Preparation and evaluation of an eco-friendly, reactive, and phytic acid-based flame retardant for wool. *React. Funct. Polym.* **134**, 58–66.
- Cheng, X.-W., Wang, Z.-Y., Jin, W.-J., Guan, J.-P., 2022. Covalent flame-retardant functionalization of wool fabric using ammonium phytate with improved washing durability. *Ind. Crops Prod.* **187**, 115332.
- Daneluti, A.L.M., Matos, J. d R., 2013. Study of thermal behavior of phytic acid. *Braz. J. Pharm. Sci.* **49**.
- Demitri, C., Sole, R.D., Scalera, F., Sannino, A., Vasapolo, G., Maffezzoli, A., Ambrosio, L., Nicolais, L., 2008. Novel superabsorbent cellulose-based hydrogels crosslinked with citric acid. *J. Appl. Polym. Sci.* **110**, 2453–2460.
- Feng, Y., Zhou, Y., Li, D., He, S., Zhang, F., Zhang, G., 2017. A plant-based reactive ammonium phytate for use as a flame-retardant for cotton fabric. *Carbohydr. Polym.* **175**, 636–644.
- Ferreira, E.S., Cranston, E.D., Rezende, C.A., 2020. Naturally hydrophobic foams from lignocellulosic fibers prepared by oven-drying. *ACS Sustain. Chem. Eng.* **8** (22), 8267–8278.
- Frone, A.N., Panaitescu, D.M., Nicolae, C.A., Gabor, A.R., Trusca, R., Casarica, A., Stanescu, P.O., Baci, D.D., Salageanu, A., 2020. Bacterial cellulose sponges obtained with green cross-linkers for tissue engineering. *Mater. Sci. Eng. C, Mater. Biol. Appl.* **110**, 110740.
- Ghanadpour, M., Carosio, F., Larsson, P.T., Wågberg, L., 2015. Phosphorylated cellulose nanofibrils: a renewable nanomaterial for the preparation of intrinsically flame-retardant materials. *Biomacromolecules* **16** (10), 3399–3410.
- Guo, Q., Cao, J., Han, Y., Tang, Y., Zhang, X., Lu, C., 2017. Biological phytic acid as a multifunctional curing agent for elastomers: towards skin-touchable and flame retardant electronic sensors. *Green. Chem.* **19** (14), 3418–3427. <https://doi.org/10.1039/C7GC01138E>.
- Jiang, G., Qiao, J., Hong, F., 2012. Application of phosphoric acid and phytic acid-doped bacterial cellulose as novel proton-conducting membranes to PEMFC. *Int. J. Hydrog. Energy* **37** (11), 9182–9192.
- Johansson, L.-S., Campbell, J.M., Rojas, O.J., 2020. Cellulose as the in situ reference for organic XPS. Why? Because it works. *Surf. Interface Anal.* **52** (12), 1134–1138.
- Kokol, V., Božić, M., Vogrinčić, R., Mathew, A.P., 2015. Characterisation and properties of homo- and heterogeneously phosphorylated nanocellulose. *Carbohydr. Polym.* **125**, 301–313.
- Liu, J., Qi, P., Meng, D., Li, L., Sun, J., Li, H., Gu, X., Jiang, S., Zhang, S., 2022. Eco-friendly flame retardant and smoke suppression coating containing boron compounds and phytic acids for nylon/cotton blend fabrics. *Ind. Crops Prod.* **186**, 115239.
- Liu, W., Shi, R., Ge, X., Huang, H., Chen, X., Mu, M., 2021. A bio-based flame retardant coating used for polyamide 66 fabric. *Prog. Org. Coat.* **156**, 106271.
- Liu, X.-h, Zhang, Q.-y, Cheng, B.-W., Ren, Y.-l, Zhang, Y.-g, Ding, C., 2018. Durable flame retardant cellulosic fibers modified with novel, facile and efficient phytic acid-based finishing agent. *Cellulose* **25**.
- Ma, Y., Luo, X., Liu, L., Zhang, C., Shang, X., Yao, J., 2021. Eco-friendly, efficient and durable fireproof cotton fabric prepared by a feasible phytic acid grafting route. *Cellulose* **28** (6), 3887–3899.
- Meftahi, A., Khajavi, R., Rashidi, A., Rahimi, M.K., Bahador, A., 2018. Preventing the collapse of 3D bacterial cellulose network via citric acid. *J. Nanostruct. Chem.* **8** (3), 311–320.

- Newman, R.H., 2004. Carbon-13 NMR evidence for cocrystallization of cellulose as a mechanism for hornification of bleached kraft pulp. *Cellulose* 11 (1), 45–52.
- Ottenhall, A., Seppänen, T., Ek, M., 2018. Water-stable cellulose fiber foam with antimicrobial properties for bio based low-density materials. *Cellulose* 25 (4), 2599–2613.
- Price, D., Anthony, G., Carty, P., 2001. 1 - Introduction: polymer combustion, condensed phase pyrolysis and smoke formation. In: Horrocks, A.R., Price, D. (Eds.), *Fire Retardant Materials*. Woodhead Publishing, pp. 1–30.
- Ren, X., Song, M., Jiang, J., Yu, Z., Zhang, Y., Zhu, Y., Liu, X., Li, C., Oguzlu-Baldelli, H., Jiang, F., 2022. Fire-retardant and thermal-insulating cellulose nanofibril aerogel modified by in situ supramolecular assembly of melamine and phytic acid. *Adv. Eng. Mater.* 24 (8), 2101534.
- Rol, F., Sillard, C., Bardet, M., Yarava, J.R., Emsley, L., Gablin, C., Léonard, D., Belgacem, N., Bras, J., 2020. Cellulose phosphorylation comparison and analysis of phosphate position on cellulose fibers. *Carbohydr. Polym.* 229, 115294.
- Schartel, B., 2010. Phosphorus-based flame retardancy mechanisms—old hat or a starting point for future development? *Materials* 3 (10), 4710–4745.
- Song, F., Zhao, Q., Zhu, T., Bo, C., Zhang, M., Hu, L., Zhu, X., Jia, P., Zhou, Y., 2022. Biobased coating derived from fish scale protein and phytic acid for flame-retardant cotton fabrics. *Mater. Des.* 221, 110925.
- Štiglic, A.D., Güreç, F., Lackner, F., Bračić, D., Winter, A., Gradišnik, L., Makuc, D., Kargl, R., Duarte, I., Plavec, J., Maver, U., Beaumont, M., Kleinschek, K.S., Mohan, T., 2022. Organic acid cross-linked 3D printed cellulose nanocomposite bioscaffolds with controlled porosity, mechanical strength, and biocompatibility. *iScience* 25 (5), 104263.
- Sun, L., Wang, H., Li, W., Zhang, J., Zhang, Z., Lu, Z., Zhu, P., Dong, C., 2021. Preparation, characterization and testing of flame retardant cotton cellulose material: flame retardancy, thermal stability and flame-retardant mechanism. *Cellulose* 28 (6), 3789–3805.
- Thota, S., Somiseti, V., Kulkarni, S., Kumar, J., Nagarajan, R., Mosurkal, R., 2020. Covalent functionalization of cellulose in cotton and a nylon-cotton blend with phytic acid for flame retardant properties. *Cellulose* 27 (1), 11–24.
- Wang, L., Lyu, W., Zhou, W., Zhang, H., 2022. The role of sodium phytate in the flotation separation of smithsonite from calcite. *Miner. Eng.* 187, 107775.
- Wang, Z., Ma, Z., Wang, S., Pi, M., Wang, X., Li, M., Lu, H., Cui, W., Ran, R., 2022. Cellulose nanocrystal/phytic acid reinforced conductive hydrogels for antifreezing and antibacterial wearable sensors. *Carbohydr. Polym.* 298, 120128.
- Watson, F.T., Smernik, R.J., Doolette, A.L., 2019. Thermal degradation of phytate produces all four possible inositol pentakisphosphates as determined by ion chromatography and <sup>1</sup>H and <sup>31</sup>P NMR spectroscopy. *Phosphorus, Sulfur, Silicon Relat. Elem.* 194 (12), 1140–1148.
- Wickholm, K., Larsson, P.T., Iversen, T., 1998. Assignment of non-crystalline forms in cellulose I by CP/MAS <sup>13</sup>C NMR spectroscopy. *Carbohydr. Res.* 312 (3), 123–129.
- Xie, X., Yuan, T., Yao, Y., Li, G., Li, Y., Wang, X., 2023. Phytic acid-based hybrid complexes for improving the interfacial property and mildew-resistance of heat-treated bamboo. *Colloids Surf. A: Physicochem. Eng. Asp.* 659, 130749.
- Yang, C.Q., Wang, X., Kang, I.-S., 1997. Ester crosslinking of cotton fabric by polymeric carboxylic acids and citric acid. *Text. Res. J.* 67 (5), 334–342.
- Yuan, H.-B., Tang, R.-C., Yu, C.-B., 2021. Flame retardant functionalization of microcrystalline cellulose by phosphorylation reaction with phytic acid. *Int. J. Mol. Sci.* 22 (17), 9631.
- Zheng, X.-T., Dong, Y.-Q., Liu, X.-D., Xu, Y.-L., Jian, R.-K., 2022. Fully bio-based flame-retardant cotton fabrics via layer-by-layer self assembly of laccase and phytic acid. *J. Clean. Prod.* 350, 131525.
- Zuckerstätter, G., Schild, G., Wollboldt, P., Röder, T., Weber, H.K., Sixta, H., 2009. The elucidation of cellulose supramolecular structure by <sup>13</sup>C CP-MAS NMR. *Lenzing Ber.* 87, 38–46.